

Article

Structure–Performance Relationship of Coal-Based Lubricating Base Oils and Sensitivities to Typical Additives

Junyi Liu ¹, Zhaojun Zhang ², Xia Zhou ¹ , Wenjing Hu ², Renmin Pan ^{1,*} and Jiusheng Li ^{2,*} 

¹ School of Chemistry and Chemical Engineering, Nanjing University of Science and Technology, Nanjing 210094, China; zhouxia@njjust.edu.cn (X.Z.)

² Laboratory for Advanced Lubricating Materials, Shanghai Advanced Research Institute, Chinese Academy of Sciences, Shanghai 201210, China; zhangzj@sari.ac.cn (Z.Z.); huwj@sari.ac.cn (W.H.)

* Correspondence: panrenming@njjust.edu.cn (R.P.); lijs@sari.ac.cn (J.L.)

Abstract: The relationship between the structure characteristics and performances of coal-based hydrogenation isomeric (CTL) base oil and metallocene-catalyzed coal-based poly-alpha-olefin (mPAO) base oil is clarified in this paper. CTL and mPAO were compared with typical petroleum-based and natural gas-based commercial API III and IV base oils. Pressurized differential scanning calorimetry (PDSC), the rotary bomb oxidation test (RBOT), and a four-ball friction tester were used to evaluate the oxidation stability and lubrication performance of base oils under different working conditions. The sensitivity of different base oils to typical antioxidants and extreme-pressure antiwear agents was compared. In particular, the composition and structure of CTL base oil are clearly different from GTL and mineral base oil. The coal-based CTL and mPAO base oils exhibit commendable viscosity–temperature properties, coupled with low-temperature fluidity, fire safety, and minimal evaporation loss. The lubricating properties, oxidation stability, and sensitivity to extreme-pressure antiwear agents of CTL are close to those of similar base oils. However, the sensitivity of CTL to typical antioxidants is relatively poor. In addition, compared with commercial PAO base oil, mPAO has a lower isomerization degree and fewer isomerization types. The oxidation stability and sensitivity to typical antioxidants of mPAO base oil are comparable with those of commercial PAO base oil, while its lubrication performance and sensitivity to typical extreme-pressure antiwear agents are significantly better than those of commercial PAO base oil.



Citation: Liu, J.; Zhang, Z.; Zhou, X.; Hu, W.; Pan, R.; Li, J. Structure–Performance Relationship of Coal-Based Lubricating Base Oils and Sensitivities to Typical Additives.

Lubricants **2024**, *12*, 156.

<https://doi.org/10.3390/lubricants12050156>

Received: 24 March 2024

Revised: 26 April 2024

Accepted: 28 April 2024

Published: 30 April 2024



Copyright: © 2024 by the authors. Licensee MDPI, Basel, Switzerland. This article is an open access article distributed under the terms and conditions of the Creative Commons Attribution (CC BY) license (<https://creativecommons.org/licenses/by/4.0/>).

Keywords: Fischer–Tropsch synthetic oil; CTL base oil; metallocene PAO; oxidation stability; additive sensitivity

1. Introduction

Lubricating oil, as the largest lubricant used in the world, is an indispensable material for equipment operation. The proportion of base oil in lubricating oil is usually more than 85%. For a long time, crude oil has been produced in various lubricant base oils [1]. Limited by crude oil quality and production process factors, it is difficult for China to produce API III and IV high-quality base oils through crude oil [2]. Recently, utilizing abundant coal resources, a Chinese company realized the conversion of coal into lubricant base oil (CTL) through a coal indirect liquefaction technology route, which is similar to that of Shell GTL (gas-to-liquid) base oil [3]. CTL and GTL are also known as Fischer–Tropsch (F-T) synthetic base oil due to their similar process. PAO base oil is obtained by the polymerization of alpha-olefins in indirect coal liquefaction products. At the same time, α -olefins may also be used to prepare other API V base oils or lubricant additives [4].

Different from the traditional petroleum base oil performances that have been fully studied [5–8], there is relatively less research on CTL base oil. CTL base oil has the characteristics of a high viscosity index, low evaporation loss, and no sulfur, nitrogen, and aromatic hydrocarbons [9,10]. CTL base oil can reach the level of PAO in terms of Noack

volatility, antioxidant properties, and thermal stability, while PAO only maintains certain advantages in extreme-low-temperature fluidity. The excellent physical and chemical properties of CTL base oil make it show good application prospects in emerging fields, such as electric vehicles, power batteries, data-center-direct liquid cooling, and so on.

Additives are used as components to improve or compensate for the performance of base oil. Adding suitable lubricating oil additives to CTL can give full play to its performance advantages. The sensitivity of base oil to additives is directly related to the use effect and economy of base oil. Hui et al. [11] studied the oxidation stability of CTL base oil by the PDSC method. They showed that the oxidation stability and sensitivity to antioxidants of CTL base oil are between API III and IV. For GTL base oil, An et al. [12] and Liang et al. [13] studied the sensitivity of antioxidant and antiwear additives of GTL. However, there is still a lack of performance comparison between petroleum-based oil and PAO. Based on the performance characteristics of CTL, there is relatively more research focus on the application of CTL base oil, such as in rolling [14], gasoline engines [15], and diesel engines [16], which has promoted the practical application of CTL base oil. However, the structure and composition of base oil are the internal factors that affect its performance. However, there is currently limited research on CTL at the molecular scale. To reveal the relationship between the structure of CTL base oil and the viscosity index from a molecular perspective, Zhang et al. [17] characterized its molecular structure using ^{13}C NMR spectrums. From the correlation analysis, normal paraffin, average chain length, and 6- or 7-methyl-substituted are the key factors for the high viscosity index of CTL base oils, and the increase in other branched-chain structure contents will reduce the viscosity index. For the oxidation resistance of CTL, Yu et al. [18] studied the effect of antioxidant additives on the thermal oxidation performance of CTL base oil by test and molecular dynamics simulation. As known, CTL, GTL, and API III base oils are all hydrogenated isomeric base oils, while the differences between CTL base oil and other base oils from a molecular perspective are still unknown. Therefore, it is of great scientific significance to study the relationship between the structure and properties of different base oils.

PAO base oil has an excellent comprehensive performance. At present, the research on PAO base oil prepared from coal-based α -olefin is mainly carried out from the aspect of the polymerization process and laboratory product performance. Wu et al. [19,20] investigated the process conditions for synthesizing low-viscosity PAO base oil with coal-based α -olefins using AlCl_3 as a catalyst. The authors [21] and Ma et al. [22,23] designed a new metallocene catalyst. It is the first in the world to prepare low-viscosity metallocene PAO (mPAO) base oil from coal-based α -olefins. The properties of mPAO8 synthesized in the laboratory were preliminarily studied. The results show that the oxidation stability, antioxidant sensitivity, pour point, and Noack evaporation loss of mPAO8 were similar to those of commercial products. MPAO8 has a high viscosity index, flash point, and thermal stability. Antioxidants can significantly improve the antioxidant activity of mPAO8.

Coal-based CTL and mPAO base oils are new high-quality base oils prepared with new raw materials and processes. It is key to realize the rational utilization of coal-based base oil to clarify its composition, structure, and performance differences from traditional mineral-based API III and IV base oils. However, it is regrettable that there is no systematic and comprehensive research and comparison between coal-based base oil and traditional base oil. Meanwhile, the current research on coal-based low-viscosity mPAO base oil is limited to the performance research of laboratory synthetic products. During the industrialization of the catalytic process, enlargement of the reaction vessel will affect the polymerization process, which will affect the performance of mPAO base oil. Therefore, it is necessary and meaningful to study commercial coal-based low-viscosity mPAO.

In this work, 4.0cSt CTL and mPAO base oil, GTL base oil, and typical commercial petroleum-based API III and IV base oils with the same viscosity were selected as the research objects. The composition and structure of the above base oils were characterized by NMR, GPC, and GC, and efforts were made to establish the relationship between the structure and performance of the base oils. At the same time, the physicochemical

properties, lubricating properties, oxidation stability, and sensitivity to typical antioxidants and extreme-pressure antiwear agents of the above base oils were compared, helping to better understand the performance characteristics exhibited by CTL and mPAO base oils derived from coal. By studying the molecular structure of base oils, the structural characteristics of different base oils can be identified. This guides the molecular design and simulation of subsequent special additives for new base oils (such as Fischer–Tropsch synthetic base oils). Research on the sensitivity of base oil antioxidants and lubricating additives can guide the selection of antioxidant type and dosage when developing different base oil formulations to develop lubricants with better performance.

2. Materials and Methods

2.1. Materials

Five low-viscosity base oils with a viscosity of 4.0cSt were selected as the representative base oils from different raw materials. CTL4 is a coal-based hydroisomerization base oil. mPAO4 base oil is a low-viscosity PAO4 base oil industrially produced by the polymerization of coal-based C10 α -olefins with a metallocene catalyst. Figure 1 is a schematic diagram of the process route for CTL4 and mPAO4. In this paper, both CTL4 and mPAO4 were provided by Shanxi Lu'an Taihang Lubrication Technology Co., Ltd. (Changzhi, China).

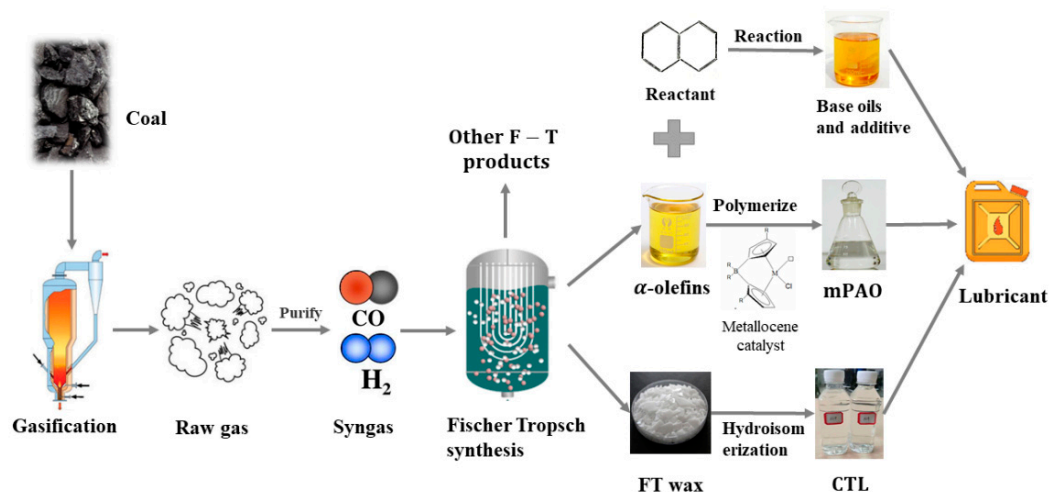


Figure 1. Technical route of coal-to-lubricant base oil.

Compared with CTL4, Shell's natural gas-based lube base oil (GTL4) and petroleum-based API III oil (YU4) were selected. For comparison with mPAO4, commercially available PAO4-M was prepared from petroleum-based C10 α -olefin polymerization.

As shown in Table 1, 3 typical commercial antioxidants were selected for the experiment, namely, thioester (AO1), phenolic (AO2), and arylamine (AO3) antioxidants. They were added to the test oils at 0.5 wt% to investigate the sensitivity of different base oils to the antioxidants. Sulfide isobutylene (EP, produced by Henan Runyang New Chemical Materials Co., Ltd. (Puyang, China)), alkyl phosphate (AW1, produced by Huihua Technology Co., Ltd. (Zibo, China)), ZDDP (AW2, produced by Huihua Technology Co., Ltd.), and alkyl phosphate amine salt (AW3) were selected as typical representatives of extreme-pressure antiwear agents. The differences in the sensitivity of different base oils to typical extreme-pressure antiwear agents were investigated at 1.0 wt%.

Table 1. Additives for testing.

Code	Name or Structure
AO1	Thioester, Vanlube 7723
AO2	Phenolic, Irganox L135
AO3	Arylamine, Irganox L57
EP	Sulfurized isobutylene (sulphur content 40–45%)
AW1	Tricresyl phosphate, TCP
AW2	Zinc dialkyldithiophosphate, ZDDP
AW3	Amine phosphates, Vanlube 672

2.2. Structural Characterization of Base Oil

Gas chromatography was used to test the component distribution of 5 base oils. The gas chromatograph (GC) instrument model was an Agilent HP-7890B. The detector was a hydrogen ion flame detector. The procedure for the temperature heating process was as follows: firstly, it is constant at 50 °C for 2 min, and then, it rises to 350 °C at a rate of 5 °C/min and keeps at 350 °C for 30 min.

Gel permeation chromatography (GPC) was used to characterize the molecular weight distribution of 5 base oils. The instrument model was a Malvern Panalytical Viscotek GPC-MAX (Worceterhire, UK). An automatic sampler with a fixed 200 µL-volume variable-spray syringe was used. The syringes were cleaned twice with solvent before each sampling. The detector and autosampler were controlled by a Dell computer running Omniscan 4.2 software.

The ¹³C and ¹H NMR spectra were recorded on a Zhongke Niujiu WNMRI-400 NMR (Wuhan, China) spectrometer operating at 400.17 MHz for ¹H and 100.62 MHz for ¹³C using a multinuclear 5 mm probe [24]. Solutions of base oil (50 wt%) were prepared in CDCl₃ containing 10% Tetramethylurea (TMU). The testing conditions for ¹³C NMR spectra were as follows: a pulse width of 3.1 µs, a chamfer angle of 30°, a spectral width of 11,160.7 Hz, an observed nuclear resonance frequency of 400 MHz, a sampling time of 1.0 s, a delay time of 5 s, a sampling frequency of 5 k, and deuterated chloroform lock-in. Quantitative ¹³C NMR spectra were recorded under reverse-gated conditions.

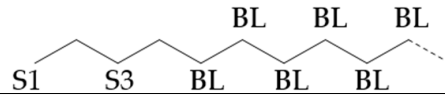
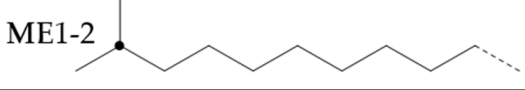
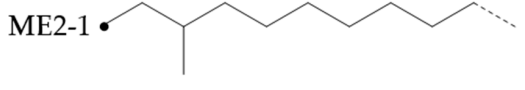
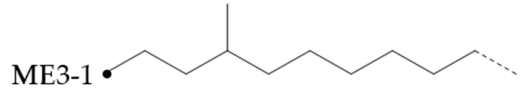
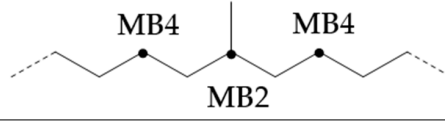
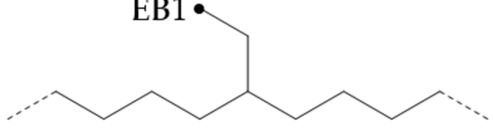
According to the ¹H NMR spectrum and integral curve, the area integration counts of the proton peaks of methyl (-CH₃), methylene (-CH₂), and secondary methyl (-CH) were calculated to obtain the branching degree (BI) of the specimen. The branching degree (BI) was calculated according to the following formula:

$$BI = \frac{\frac{1}{3}A_{(CH_3)}}{\frac{1}{2}A_{(CH_2+CH)}} \quad (1)$$

In the formula, $A_{(CH_3)}$ is the methyl proton peak (δ : 0.2–0.85) area, and $A_{(CH_2+CH)}$ is the proton peak of methylene and the methylene (δ : 0.85–2.4) area integral count.

Assuming that all base oils have only short methyl- or ethyl branching, the isomeric carbon atoms have an effect on the chemical shifts of the four nearby carbons. In combination with Reference [25], the types of carbon atoms in base oil molecules corresponding to the ¹³C NMR chemical shifts were classified. To ensure accurate and proportional integration, all signals in all ¹³C NMR were normalized with the signal of TMU methyl at 38.41 ppm as 100, and the spectrum was integrated according to the chemical shifts listed in Table 2. The integral area of each peak was normalized by the peak of TMU methyl at 38.41 ppm as 1.0.

Table 2. Carbon atom position in base oil molecule corresponding to ^{13}C chemical shift.

	δ/ppm	Carbon Atom Position [25]
ALL	5~50	
TMU	38.41	-
S1	14.1	
S3	32.1	
BL	29.7	
ME1-2	28	
ME2-1	11.3	
ME3-1	14.4	
MB2	32.8	
MB4	27.1	
EB1	10.7	
MB ALL	19.0~20.5	All methyl chains

The amount of long unbranched carbon in base oil molecules can be estimated by signals from unbranched carbon. The long linear chain itself (BL) requires that the carbon be surrounded by at least three unbranched CH_2 carbon in two directions. In addition, the S3 signal can be used to indicate the long unbranched end chain because it requires at least 6 nearby carbons to be unbranched. Therefore, the amount of long unbranched-carbon segments can be calculated by the following formula:

$$A_{BLC} = A_{BL} + A_{S3} \quad (2)$$

By integrating the characteristic methyl region (δ : 19.0~20.5), the number of methyl-branched chains inside the carbon chain can be easily determined, which includes all methyl-branched chains on the carbon chain. Therefore, the signal of the methyl-branched chain (A_{MeB}) in all base oils can be calculated by the following formula:

$$A_{MeB} = A_{MB\text{ ALL}} + A_{ME1-2} + A_{ME2-1} \quad (3)$$

Since there should be no longer branched chains than ethyl, the total signal (A_B) of all branched chains can be easily determined by adding the signals A_{EB1} of the ethyl-branched chains:

$$A_B = A_{MeB} + A_{EB1} \quad (4)$$

Then, the percentage of carbon chain methylation branches P_{MeB} can be determined:

$$P_{MeB} = \frac{A_{MeB}}{A_B} \times 100\% \quad (5)$$

The methyl-branched chain at the end of the chain (A_{MBE}) can be estimated by adding the signals from all the me series structures:

$$A_{MBE} = A_{ME1-2} + A_{ME2-1} + A_{ME3-1} \quad (6)$$

The methyl branch chain in the middle of the chain can be represented by A_{MB2} . The methyl branch position can be expressed by calculating the percentage of methyl branches at the end of a base oil molecule:

$$P_{MBE/MB} = \frac{A_{MBE}}{A_{MBE} + A_{MB2}} \times 100\% \quad (7)$$

If a branch (or any other structure) is close enough to the methyl branch (MB Series) in the carbon chain, it will change the chemical shift of the adjacent carbon from the farthest carbon (MB5). With the change in chemical shift, the signals from these carbons are not included in the MB Series integral. This also means that the change in the MB Series signal strength can indirectly detect the presence of nearby structures. For example, if a structure is close enough to change the displacement of MB4 without changing the displacement of MB2, the amount of MB4 signal observed is less than that of the MB2 signal. Ideally, the ratio of MB2 and MB4 signals should be 1:2 (due to symmetry, each MB2 carbon corresponds to two MB4 carbon), so any change in this ratio can be attributed to nearby interference structures, and it is not even necessary to know the exact structure involved. This can be expressed as calculating the “lost” mb4 signal as a percentage of the MB2 signal:

$$P_{MBDiff} = \frac{A_{MB2} - A_{MB4} \times 0.5}{A_{MB2}} \times 100\% \quad (8)$$

Therefore, this parameter represents the possibility of the existence of a structure near the methyl branch and can be considered as measuring the “purity” of the methyl branch. A lower value means that the methyl branch is well separated from other structures, while a higher value indicates that, in many cases, there are methyl branches or other structures nearby.

2.3. Physicochemical Properties

Standard methods, such as ASTM D445 [26], ASTM D2270 [27], ASTM D92 [28], ASTM D5950 [29], ASTM D5293 [30], and ASTM D5800 [31], were used to test the kinematic viscosity, viscosity index (VI), flash point, pour point, $-30\text{ }^{\circ}\text{C}$ low-temperature dynamic viscosity (CCS), and NOACKevaporation loss of base oils to compare the physicochemical properties of different base oils.

2.4. Oxidation Stability

The oxidation stability of the base oil and antioxidant-containing samples was measured using a pressurized differential scanning calorimetry (PDSC) from Switzerland’s METTLER TOLEDO company (Greifensee, Switzerland). The initial oxidation temperature (IOT) of oil products was measured using the programmed heating method. The test conditions were a heating rate of $10\text{ }^{\circ}\text{C}/\text{min}$, oxygen pressure of 3.5 MPa, oxygen flow rate of 100 mL/min, open aluminum dish diameter of 6 mm, and sample size of 3.0 mg, and the initial oxidation temperature was taken as the temperature of the severe oxidation of the oil. The ASTM D6186 [32] constant-temperature method was used to determine the oxidation induction time (OIT) of the oil products. The test conditions were a constant temperature of $160\text{ }^{\circ}\text{C}$, oxygen pressure of 3.5 MPa, and oxygen flow rate of 100 mL/min. The time for the oil to undergo severe oxidation under this temperature condition was tested.

The rotary bomb oxidation test (RBOT) was employed using P/N15200-3 from SETA (London, UK). For the base oil, the use of copper wire and water in the ASTM D2272 [33] method has a significant catalytic effect on the oil, resulting in insignificant differences in the test results between different oils. Considering that there is often contact with metallic

iron during the actual work process, this article improved the ASTM D2272 method. The specific improvement method is to replace the copper wire in the ASTM D2272 method with a steel ball, which is made of bearing steel (GB/T 308.1-2013 [34] medium high-carbon chromium bearing steel ball), with a diameter of 12.7 mm and no longer adding water as a catalyst in the projectile. The projectile is oxygenated at a pressure of 620 kPa, tested at a temperature of 150 °C, and rotated at a speed of 100 r/min. The time from the beginning of the experiment to a pressure drop of 175 kPa is the RBOT oxidation induction period.

2.5. Friction and Wear Test

The friction and wear performance of different base oils and oils containing extreme-pressure antiwear additives were tested using a four-ball friction tester. The instrument used in the experiment was the MS-10A lever-type four-ball friction testing machine, with a maximum speed of 3000 rpm. The experimental steel ball was a GCr15 steel ball produced by Falex Company in the United States, with an average hardness of 66.1 HRC and a diameter of 12.7 mm.

GB/T 3142 [35] was used to test the last nonseizure load (PB) and weld point (PD) of oil containing extreme-pressure agents to compare the sensitivity of different base oils to extreme-pressure agents.

The antiwear performance of lubricants containing different extreme-pressure antiwear agents was tested using the SH/T 0198 method. Considering the load-bearing capacity of the selected additive, the load for most experiments was 196 N at 75 °C for 60 min and at a rotational speed of 1200 rpm. After the experiment, the diameter of the wear marks WSD_{196}^{1200} was observed under an electron microscope. Under constant speed conditions, the lubrication state of the lubricant is relatively stable and single. In order to comprehensively investigate the lubrication performance of the base oil under different lubrication states, the speed of the four-ball friction testing machine was controlled by code to increase from 0 to 2800 rpm at a rate of 20 rpm per 0.5 min. Other conditions were the same as those of the constant-speed test. The diameter of the wear marks after the test was recorded as WSD_{196}^{0-2800} . Due to the good antiwear performance of amine phosphates, which mainly act as a friction modifier under a load of 196 N, larger test load conditions of 392 N and 785 N were added to investigate antiwear performance in different base oils.

According to the principle of the Stribeck curve [36], in the process of a variable-speed test, the lubricant is in a boundary lubrication state at low speed. With the increase in speed, the lubricant film thickness increases, and the lubrication state changes from boundary lubrication to elastohydrodynamic lubrication. With a further increase in speed, the enhanced shear effect of the contact surface and the heat generated by friction leads to the transformation of the lubricant from Newtonian fluid to non-Newtonian fluid [37,38], thus reducing the bearing capacity of the lubricant. Therefore, during the variable-speed test of different base oils, the friction coefficient curve generally shows a trend of first decreasing and then increasing.

3. Results and Discussion

3.1. Structure and Property Relationship of Coal-Based Base Oil

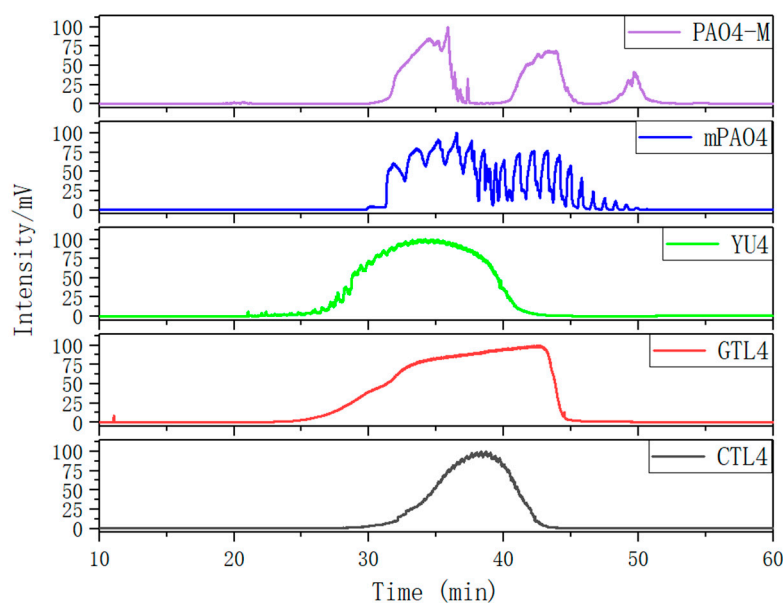
The results of the physical and chemical properties of different base oils are shown in Table 3. CTL4 has a high viscosity index and flash point and low evaporation loss for hydroisomerization base oils of about 4.0cSt. The higher viscosity index indicates that the viscosity of CTL4 is less sensitive to temperature changes. The high flash point indicates that CTL4 has good safety. The low evaporation loss indicates that CTL4 is not easy to evaporate at high temperatures. The pour point of CTL4 is significantly lower than that of the mineral base oil but 6 °C higher than that of GTL4. The low-temperature dynamic viscosity (CCS) at 30 °C reflects the low-temperature fluidity of oil products. CTL4 has obvious advantages over the mineral base oil in low-temperature fluidity and is slightly better than GTL4.

Table 3. Test results of different base oil physicochemical properties.

	CTL4	YU4	GTL4	mPAO4	PAO4-M
Kinematic viscosity/mm ² ·s ⁻¹					
40 °C	17.33	18.99	18.44	16.73	18.73
100 °C	3.97	4.12	4.063	3.85	4.12
VI	128	119	121	125	122
Flash point/°C	233	225	224	212	202
Pour point/°C	−33	−21	−39	−75	−66
CCS (−30 °C)/mPa·s	1018	1421	1177	902	921
NOACK evaporation loss (250 °C, 1 h)/%	11.8	15	12.4	12.1	12.9

For PAO base oil, the viscosity index, flash point, evaporation loss, and −30 °C low-temperature dynamic viscosity of mPAO4 were slightly better than those of commercial PAO4, but the pour point of mPAO4 was significantly lower than that of commercial PAO4. In general, coal-based base oils show certain advantages over mineral- and natural gas-based base oils in viscosity–temperature performance, low-temperature fluidity, and evaporation loss.

Figure 2 shows the gas chromatographic (GC) curves of different base oils after normalization. The GC curves of three kinds of 4.0cSt hydroisomerization base oils present a single peak form, which indicates that the boiling points of the components in the base oil are continuously distributed. The peak width of CTL4 is significantly smaller than that of GTL4 and YU4, indicating that the components of CTL4 are more concentrated. Compared with CTL4, the content of the low-boiling-point components of YU4 and GTL4 is higher, which is the reason for their low flash point and high evaporation loss.

**Figure 2.** Gas chromatogram of different base oils.

The GC curves of the two PAO base oils show a multi-peak form. According to the carbon number law and boiling-point law of gas chromatography [39], a large number of experiments have proved that at a certain temperature, the logarithm of the adjusted retention time of homologs has a linear relationship with the number of carbon atoms in the molecule (carbon atoms > 3). At the same time, the logarithm of the adjusted retention time of isomeric compounds with the same carbon-number carbon chain in the same family is linear with their boiling points. Therefore, for the GC of the hydrocarbon base oil, the higher the carbon number and boiling point of the corresponding component correlate with the

increase in retention time. The GC of mPAO4 consists of two large peaks, which contain several small peaks. Two big peaks represent the trimer and tetramer of α -olefins. The small peaks that make up the trimer and tetramer peaks are molecules with different isomeric forms under the degree of polymerization. MPAO4 has fewer molecular isomerization forms of the same polymerization, which leads to obvious differences in boiling points between molecules. This results in the GC curve exhibiting multiple small peaks. However, PAO4 prepared with a non-metallocene catalyst has more isomerization forms, which makes the difference in boiling points of the same polymerization molecules not obvious. This results in a smoother GC curve. The third small peak of the PAO4-M curve is pentamer. Since mPAO4 does not contain pentamer, its kinematic viscosity is slightly lower than that of PAO4-M, and its pour point and low-temperature fluidity are better.

The molecular-weight test results of different base oils by GPC are in Table 4. The separation mode of GPC is not based on molecular weight but on the volume of polymers in solution. Therefore, it is difficult to test the molecular weight of polymers with a molecular weight less than 1000. However, the molecular weight obtained by the GPC test can indirectly reflect the volume of base oil in the solution. In Table 4, due to the existence of pentamer, the number of average Mn and weight-average molecular weights (Mw) of commercially available PAO4-M are significantly greater than those of mPAO4. This indicates that the molecular cluster volume of PAO4-M in solution is larger. The molecular weight distribution of commercially available PAO4-M is wider, which is consistent with the information obtained by GC.

Table 4. GPC test results of base oils.

	CTL4	YU4	GTL4	mPAO4	PAO4-M
Mn	872	721	838	885	975
Mw	923	788	891	958	1075
Mw/Mn	1.058	1.092	1.064	1.083	1.103

For hydroisomerization base oils, it can be found that the molecular weight distribution of CTL4 is narrower, and the average molecular weight is relatively larger. This is due to fewer light components and a more concentrated distribution of components. YU4 has the lowest average molecular weight and wide molecular weight distribution due to the large amount of its light components. GTL4 has more high-boiling-point components than CTL4 and YU4, but its low-boiling-point components are higher than CTL4. This leads to GTL4's molecular weight being slightly less than CTL4, and its molecular weight distribution is wider than CTL4.

Table 5 summarizes the results of ^1H NMR and ^{13}C NMR spectra. The BI of hydroisomerization base oils is about 10.0% higher than that of PAO base oil. This indicates that the isomerization degree of hydroisomerization base oil is high. Combined with the VI of base oils, it was found that the VI of base oils is negatively correlated with the branching degree (BI), whether it is hydroisomerization base oils or PAO base oils. However, YU4 is an exception. This may be related to its special branching form and location.

The content of nonbranched-carbon A_{BLC} in PAO is higher than that in hydroisomerization base oil. A_{MeB} is the statistical value of methyl-branching content in base oil molecules. It was found that the A_{MeB} of hydroisomerization base oils is significantly higher than that of PAO base oils. The above structural statistical results once again prove that the isomerization degree of the hydroisomerization base oil was greater than that of PAO base oil, which is consistent with the BI-value test results. The base oil with a high isomerization degree of hydrocarbon base oil may show better solubility of additives.

In the hydroisomerization base oils, the content of nonbranched-carbon A_{BLC} of YU4 is significantly higher than that of CTL4 and GTL4, and the A_{BLC} value of CTL4 is slightly higher than that of GTL4. However, it is strange that the A_{MeB} of the CTL4 base oil is also larger than that of GTL4. It is not as significantly smaller than GTL4 as YU4. This indicates that CTL4 contains a high methyl content and branched-carbon content at the same time.

When the total carbon content of all base oils is basically the same, it means that there are fewer other branched forms of CTL4. From the content of ethyl-branched EB1 of different base oils, EB1 of CTL4 is slightly smaller than that of GTL4. At the same time, the BI of GTL4 is higher, but the A_B is less than that of CTL4, indicating that there are branches that are not counted, for example, ethyl branching near the end of the chain. Further, the proportion of methylated branches P_{MeB} in the CTL4 base oil is also slightly higher than that in GTL4. In terms of the proportion of the chain-end branching $P_{MBE/MB}$ of different base oils, the $P_{MBE/MB}$ of CTL4 and YU4 at the end of the chain is significantly less than that of GTL4. P_{MBDiff} represents the degree of other branching near the methyl branching of the chain. For isomerization and hydroisomerization base oil, the P_{MBDiff} value of YU4 is high. It shows that there are more other branches around the methyl chain, indicating that the branching aggregation degree is high. However, the P_{MBDiff} value of GTL4 is 0, indicating that there is no effect of other structures near the methylation of its chain. Its chain-branching density is low. The branch on the long-branched chain can improve the low-temperature fluidity of base oil.

Table 5. NMR results of different base oils.

	CTL4	YU4	GTL4	mPAO4	PAO4-M
ALL	14.7	14.16	14.72	14.87	14.71
TMU	1	1	1	1	1
S1	0.67	0.67	0.79	1.72	1.72
S3	0.34	0.41	0.38	1.41	1.2
BL	1.74	2.09	1.5	1.69	2.17
ME1-2	0.13	0.1	0.13	0.02	0.13
ME2-1	0.14	0.11	0.15	0	0.01
ME3-1	0.14	0.1	0.13	0.02	0.07
MB2	0.42	0.36	0.31	0.03	0.03
MB4	0.8	0.57	0.62	0.28	0.08
EB1	0.21	0.1	0.22	0	0.01
MB ALL	1.06	0.77	0.99	0.09	0.04
BI/%	24.66	25.61	27.23	17.30	20.48
A_{BLC}	2.08	2.5	1.88	3.1	3.37
A_{MeB}	1.33	0.98	1.27	0.11	0.18
A_B	1.54	1.08	1.49	0.11	0.19
P_{MeB}	86.36%	90.74%	85.23%	100.00%	94.74%
$P_{MBE/MB}$	49.40%	46.27%	56.94%	57.14%	87.50%
P_{MBDiff}	4.76%	20.83%	0.00%	−366.67%	−33.33%

The following results are based on the structural analysis of different hydroisomerization base oils. Compared with GTL4, the overall branching degree of CTL4 is slightly lower, and the content of unbranched carbon in the molecule is higher. The CTL4 branched form is less and mainly methyl-branched, while other branched forms are less. In terms of branching position, CTL4 has less branching at the end of the chain, and the branching concentration is slightly higher than that of GTL4. The branching degree of YU4 is much less than that of GTL4 and CTL4, and there are a large number of unbranched carbon in the molecule. The main form of branching is dense methyl branching. According to the analysis results of the rheological properties of different isomeric alkanes in Reference [40], the molecular pour point of isomeric alkanes with the long unbranched length of the main chain is generally poor. This is the reason why the pour points of different base oils are $YU4 > CTL4 > GTL4$, and YU4 has poor low-temperature fluidity. Although the branchless-carbon content of the two PAO base oils is high, the molecular configuration of the PAO base oils is a long-branched star structure, so they still have good low-temperature fluidity.

In PAO base oils, the methyl-branched chain content of mPAO4 A_{MeB} was slightly less than that of commercial PAO4-M, which was consistent with the phenomenon reflected by gas chromatography and the branching degree (BI). According to P_{MeB} , the branched form of PAO base oil is mainly methyl-branched; in particular, mPAO4 does not contain

ethyl-branched chains. By comparison, it was found that the percentage of terminal methyl branches $P_{MBE/MB}$ of commercial PAO4-M was higher than that of mPAO4, indicating that the isomerization position was mainly at the end of the chain. As the branching of PAO base oil mainly occurs at the end of the chain, the content of MB2 is low, and the content of MB4 is high due to the influence of skeleton carbon, so the negative value of P_{MBDiff} has no practical significance. Due to the use of new catalysts, mPAO4 has the characteristics of a low degree of isomerization and few isomerization forms. The structure of mPAO4 is more regular, so it has better performance.

3.2. Oxidation Stability of Base Oil

Table 6 shows the test results of the oxidation stability of different base oils using PDSC and the RBOT. When the base oil is not added, the oxidation stability of several base oils under different test conditions has little difference. Among them, the oxidation stability of the petroleum-based YU4 is relatively good because it is difficult to remove a small amount of aromatic compounds in the preparation process. Aromatic compounds have certain antioxidant properties. Therefore, the YU4 base oil has good oxidation stability.

Table 6. Oxidation stability of different base oils.

	CTL4	YU4	GTL4	mPAO4	PAO4-M
IOT/°C	198.53	201.5	198.08	199.58	201.78
OIT (160 °C)/min	9.04	9.86	8.83	9.14	8.92
RBOT/min	29.2	39.8	35.9	29.2	32.0

3.3. Sensitivity Performance of Different Base Oils with Antioxidants

Table 7 shows the sensitivity comparison of different base oils to the thioester-type antioxidant (AO1). It was found that the IOT of the above base oils added with the 0.5 wt% AO1 antioxidant has no significant change compared with the base oil under the PDSC temperature program test condition. However, under the constant-temperature test condition of 160 °C, the OIT of most base oils except CTL4 increased significantly, indicating that CTL4 has poor sensitivity to the thioester antioxidant. For the base oil other than CTL4, the OIT increased by at least one time after adding the 0.5 wt% AO1 antioxidant, and the OIT of mPAO4 containing 0.5 wt% AO1 is 110.94 min, which is much greater than that of PAO4-M, indicating that mPAO4 has good sensitivity to the thioester antioxidant.

Table 7. Sensitivity of different base oils to thioester-type (AO1) antioxidant.

	0.5 wt% AO1				
	CTL4	YU4	GTL4	mPAO4	PAO4-M
IOT/°C	201.1	198.5	205.8	196.3	196.6
OIT (160 °C)/min	11.2	29.0	25.1	110.9	28.4
RBOT/min	107.3	1524.6	499.8	342.5	373.7

It was found that the RBOT duration of base oils increases to varying degrees, indicating that the antioxidant played a role under the test conditions. Among them, the RBOT duration of CTL4 increases slightly, indicating that its sensitivity to AO1 is weak. The RBOT duration of the two PAOs is significantly longer than that of CTL4, both of which are about 360 min, indicating that the sensitivity of the two PAOs to the AO1 antioxidant is similar. Compared with the base oil, the RBOT duration of GTL4 and YU4 reaches about 500 min and 1500 min, respectively, indicating that GTL4 and YU4 have better sensitivity to AO1, and YU4 has the most prominent sensitivity. The above test results show that for the same antioxidant, different base oils and service conditions have significant effects on performance.

Table 8 shows the sensitivity comparison of different base oils to the phenolic (AO2) antioxidant. It was found that the initial oxidation temperature (IOT) of the above base

oils added with the 0.5 wt% AO2 antioxidant is significantly higher than that of the base oils under the PDSC temperature program test. Under the condition of a constant-temperature test at 160 °C, the OIT of all base oils increases significantly. However, the increase in the oxidation induction period of the two PAO base oils is more obvious, which indicates that PAO base oils are more sensitive to the phenolic antioxidant. Among the hydroisomerization base oils, YU4 has the best sensitivity to AO2, followed by CTL4 and GTL4.

Table 8. Sensitivity of different base oils to phenolic (AO2) antioxidant.

	0.5 wt% AO2				
	CTL4	YU4	GTL4	mPAO4	PAO4-M
IOT/°C	208.3	214.7	211.8	211.5	211.0
OIT (160 °C)/min	53.9	65.8	44.5	95.9	92.2
RBOT/min	323.2	5979.1	701.0	4193.2	4262.9

Under the optimized RBOT conditions, the RBOT duration of several base oils containing the 0.5 wt% phenolic antioxidant is significantly increased. The duration of the RBOT of YU4, mPAO4, and PAO4-M is up to 4000~6000 min, while the RBOT of CTL4 and GTL4 is less than 1000 min, at about 300 min and 700 min. The above phenomenon shows that CTL4 and GTL4 have poor sensitivity to the phenolic antioxidant.

Table 9 shows the sensitivity comparison of different base oils with the amine-type (AO3) antioxidant. It was found that the IOT of the above base oils added with the 0.5 wt% AO3 antioxidant is significantly higher than that of the base oils under the PDSC temperature program test. As a high-temperature antioxidant, the OIT of all base oils is significantly higher than that of base oils under the constant-temperature test condition of 160 °C and is significantly higher than that of base oils containing the 0.5 wt% phenolic antioxidant. The OIT of two kinds of PAO4 and YU4 increased more obviously, which reached more than 110 min, indicating that the sensitivity of the PAO and YU4 base oils to the amine antioxidant is more prominent. In the hydroisomerization base oil, the oxidation induction period of CTL4 and GTL4 is only about 80 min, which indicates that the sensitivity of the F-T base oil to amine antioxidants is different from that of the petroleum-based YU4.

Table 9. Sensitivity of different base oils to the amine-type (AO3) antioxidant.

	0.5 wt% AO3				
	CTL4	YU4	GTL4	mPAO4	PAO4-M
IOT/°C	216.5	214.1	215.1	216.0	218.8
OIT (160 °C)/min	76.97	114.7	85.0	130.6	123.8
RBOT/min	242.5	512.1	476.0	3912.0	5022.7

Under the optimized RBOT conditions, the RBOT duration of several base oils containing the 0.5 wt% amine antioxidant is significantly improved compared with the base oils. The time of the mPAO4 and PAO4-m RBOTs is about 4000 min and 5000 min, respectively. The performance of AO3 in mPAO4 is equivalent to that of the 0.5 wt% AO2. The performance of the high-temperature antioxidant AO3 in the same dose of PAO4-M is better than that of AO2. In the hydroisomerization base oil, the RBOT time of AO3 as a high-temperature antioxidant is significantly shorter than that of AO2. Through the comparative analysis of PDSC constant-temperature test conditions and optimized RBOT conditions, the results show that the main difference between the two is that the optimized RBOT is a fully closed system catalyzed by iron metal. The water generated by its oxidation cannot be discharged from the oxidation system. The presence of water will accelerate the formation of free radicals. However, phenolic antioxidants have a terminating effect on free radicals. Therefore, the RBOT time of base oil containing phenolic antioxidants is longer than that of amine antioxidants.

According to Table 5, the number of branched A_B chains in the YU4, mPAO4, and PAO4-M base oils is smaller than that in CTL4 and GTL4, indicating that they have less tertiary hydrogen. Tertiary hydrogen has high chemical reactivity. Therefore, base oils with fewer branches of A_B have a lower rate of generating free radicals during the oxidation process. This results in YU4, mPAO4, and PAO4-M exhibiting good sensitivity to amine and phenolic antioxidants. In particular, two types of PAO4 have better sensitivity to phenolic and amine antioxidants due to their lower A_B . However, the sensitivity of the two Fischer–Tropsch synthetic base oils to antioxidants is relatively poor.

3.4. Lubricating Performance of Different Base Oils

Table 10 shows the lubrication performance test results of different base oils. Figure 3 shows the friction coefficient curve under constant- and variable-speed test conditions. It can be seen from the data in the table that under the test conditions of 1200 rpm constant speed and 0–2800 rpm variable speed, the lubrication performance of different base oils with about 4.0cSt is clearly different. Among them, the wear scar diameter and friction coefficient of commercially available PAO4-M are large, indicating that its lubrication performance is poor. The friction coefficient of PAO4-M rises during the friction test, while other base oils are relatively stable. Under the condition of the constant-speed test, the wear scar diameters (WSDs) of coal-based CTL4 and mPAO4 are the same, but the friction coefficient of mPAO4 is the smallest among all base oils due to its increased molecular weight and regular structure. The WSDs of YU4 and GTL4 are close to each other, both of which are about 0.55 mm, and have better performance in all base oils.

Table 10. Lubricating-performance test results of different base oils.

	CTL4	YU4	GTL4	mPAO4	PAO4-M
WSD_{196}^{1200} /mm	0.627	0.541	0.555	0.625	0.806
(COF)	(0.082)	(0.071)	(0.072)	(0.064)	(0.114)
WSD_{196}^{0-2800} /mm	0.761	0.777	0.762	0.704	0.785

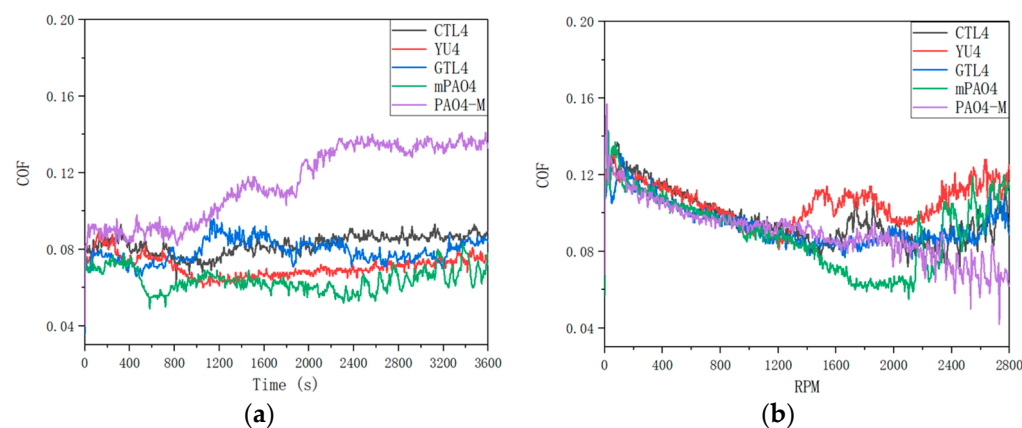


Figure 3. Friction coefficient curve of tests with different base oils: (a) 1200 rpm constant speed; (b) 0–2800 rpm variable speed.

By comparing the friction coefficient curves of different base oils (Figure 3) under variable-speed test conditions, it can be found that the variation trend of friction coefficient is basically the same before 1200 rpm, and both are linear declines. After 1200 rpm, due to less ethyl branching of YU4 and relatively small molecular volume (it can also be seen from GPC data), the thickness of the oil film formed by YU4 is insufficient. The friction coefficient curve of YU4 rises first, indicating that its shear resistance is the worst, which also leads to the increase in wear in the variable-speed test. When compared with YU4, the friction coefficient of mPAO4 base oil continues to decrease with the increase in rotating speed after 1200 rpm. The rising friction coefficient appears after maintaining the elastic

fluid lubrication state for a while, so the wear scar diameter of mPAO4 is the smallest after the test. The molecular structures of GTL4 and CTL4 are similar, so the change process of friction coefficient in the variable-speed test is similar, and the results after the test are basically the same. For PAO4-M, due to its large molecular volume, it entered the elastohydrodynamic lubrication stage with a relatively stable friction coefficient after 1200 rpm. Then, with the increase in rotating speed, the friction coefficient does not rise but decreases. This may be due to the high molecular volume of PAO4-M. With the increase in rotating speed in the process of high-speed friction, the surface wear is more likely to form an elastic fluid lubrication film after metal polishing, which makes the friction coefficient fluctuate and decrease. Similarly, the friction coefficient curves of CTL4 and mPAO4 fluctuate at high speeds.

3.5. Sensitivity Performance of Base Oil with Extreme-Pressure Antiwear Additives

Table 11 shows the sensitivity test results of different base oils containing the 1.0 wt% EP additive. The addition of the 1.0 wt% EP plays a certain antiwear protection role compared with the base oil without additives. In the constant-speed test, the wear scar diameter of GTL4 is small, which indicates that it has good antiwear sensitivity to EP. The sensitivity of mPAO4 to EP is relatively poor in the constant- and variable-speed tests. However, the WSDs of other base oils, whether the constant-speed test or variable-speed test, are relatively close after the test, indicating that the performance of EP in different base oils is basically the same. In the extreme-pressure performance test of different base oils containing the 1.0 wt% EP, the extreme-pressure additives mainly play a role in the sintering of steel balls, so the base oil has little effect on the sintering load, and there is no difference in the weld point (PD) of the different base oils. However, in the last nonseizure load PB test, different base oils showed slight differences. The PB of GTL4 and mPAO4, which performed well in the antiwear performance test, was one load level lower than that of the other base oils. In general, the sensitivity of different base oils to EP additives is different, but the difference is not significant.

Table 11. Sensitivity test results of different base oils containing EP.

	1.0 wt% EP				
	CTL4	YU4	GTL4	mPAO4	PAO4-M
WSD ₁₉₆ ¹²⁰⁰ /mm	0.424	0.442	0.398	0.459	0.430
(COF)	(0.112)	(0.094)	(0.110)	(0.103)	(0.086)
WSD ₁₉₆ ^{0–2800} /mm	0.502	0.517	0.512	0.551	0.512
PB/kg	52	52	48	52	48
PD/kg	315	315	315	315	315

Table 12 shows the sensitivity test results of different base oils containing the 1.0 wt% antiwear additive AW1. Figure 4 shows the friction coefficient curve of lubricants under constant-speed and variable-speed test conditions. The addition of the antiwear agent AW1 plays a significant antiwear role. In the constant-speed experiment, the WSDs of mPAO4 and GTL4 are significantly smaller than those of other base oils, and their friction coefficient curves are relatively stable in the experiment. In contrast, PAO4-M containing the 1.0 wt% AW1 has a larger WSD after the test, and due to the poor lubrication performance of PAO4-M base oil itself, a periodic “wear polishing” process may occur during the constant-speed test, resulting in periodic fluctuations in the friction coefficient curve. For CTL4 and YU4, their sensitivity to the AW1 antiwear agent is between that of the other base oils. It can be seen from Figure 4 that in the variable-speed test, when the speed is less than 400 rpm, the lubricant is in the running-in state, and the friction coefficient shows an upward trend with the increase in speed, and the friction coefficient of different lubricants has little difference. When the running-in is completed, the friction coefficient of the lubricant used decreases rapidly when the speed is greater than 400 rpm, and then, the friction coefficient curves

of different lubricants show different trends. The friction coefficient curves of the CTL4, GTL4, and mPAO4 base oils containing the 1.0 wt% AW1 antiwear agent decrease steadily with the speed, while the friction coefficient curves of YU4 and PAO4-M show a fluctuating upward trend. After the test, the balls' wear scar diameters of the CTL4, GTL4, and mPAO4 base oils containing the 1.0 wt% AW1 antiwear agent were significantly smaller than that of YU4 and PAO4-M, indicating that the CTL4, GTL4, and mPAO4 base oils have better sensitivity to AW1.

Table 12. Sensitivity test results of different base oils containing antiwear additive AW1.

	1.0 wt% AW1				
	CTL4	YU4	GTL4	mPAO4	PAO4-M
$WSD_{196}^{1200} / \text{mm}$	0.420	0.395	0.350	0.341	0.480
(COF)	(0.112)	(0.122)	(0.092)	(0.094)	(0.096)
$WSD_{196}^{0-2800} / \text{mm}$	0.307	0.418	0.292	0.308	0.465

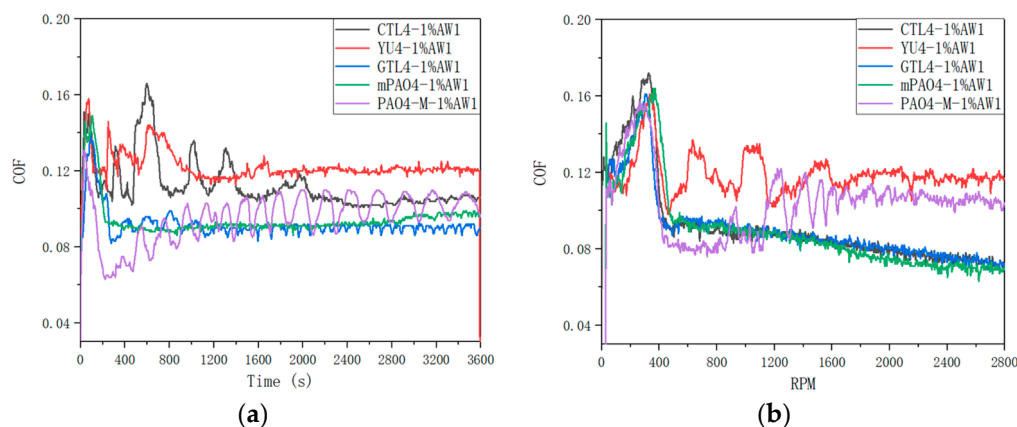


Figure 4. Friction coefficient curve of different base oils containing 1.0 wt% AW1: (a) 1200 rpm constant speed; (b) 0–2800 rpm variable speed.

Table 13 shows the sensitivity test results of different base oils containing the 1.0 wt% antiwear agent AW2. Figure 5 shows the friction coefficient curve of lubricants under constant-speed and variable-speed test conditions. The addition of the antiwear additive AW2 plays a significant antiwear role. Under the condition of a constant-speed test, the sensitivity of different base oils to AW2 is positively correlated with the lubrication performance of the base oil itself. PAO4-M has the worst sensitivity to AW2. YU4 and GTL4 have the best sensitivity to AW2. CTL4 and mPAO4 have much better sensitivity to AW2 than PAO4-M but not as good as YU4 and GTL4. In the variable-speed test, the sensitivity of different base oils to AW2 is consistent with that in the constant-speed test. The sensitivity of CTL4 and mPAO4 to AW2 is significantly better than PAO4-M but less than YU4 and GTL4. It is worth noting that from the antiwear performance data shown in Table 13 and the friction coefficient curve shown in Figure 5, AW2, as a typical antiwear agent that has been used in petroleum base oil for decades, shows excellent antiwear- and friction-reducing effects in the petroleum base oil YU4, while the antiwear- and friction-reducing effect in the other synthetic base oils is far less than YU4. On the one hand, it reveals the necessity of developing synthetic lube base oil, and, on the other hand, it also reminds us that the lubricating additives or compounding agents developed in petroleum base oil may not be able to perform as well in synthetic base oil as in petroleum-based.

Table 13. Sensitivity test results of different base oils containing antiwear additive AW2.

	1.0 wt% AW2				
	CTL4	YU4	GTL4	mPAO4	PAO4-M
$WSD_{196}^{1200} / \text{mm}$ (COF)	0.418 (0.104)	0.270 (0.082)	0.297 (0.104)	0.419 (0.114)	0.537 (0.116)
$WSD_{196}^{0-2800} / \text{mm}$	0.516	0.312	0.379	0.549	0.606

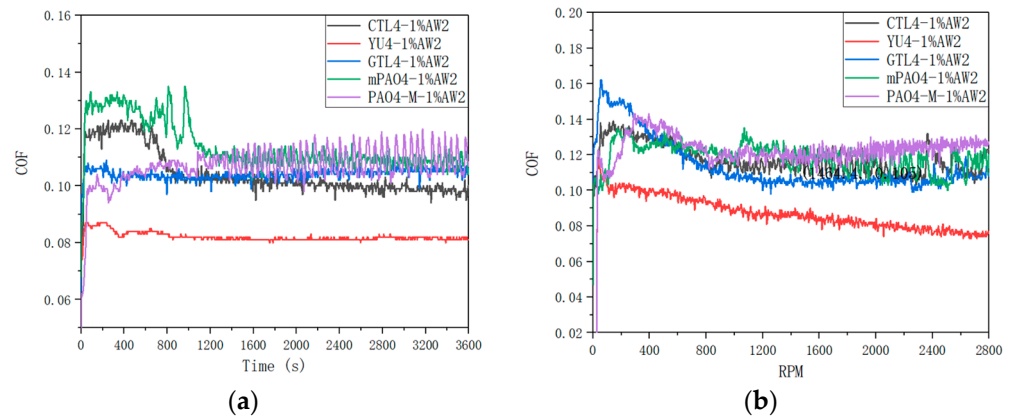


Figure 5. Friction coefficient curve of different base oils containing 1.0 wt% AW2: (a) 1200 rpm constant speed; (b) 0–2800 rpm variable speed.

Table 14 shows the sensitivity test results of the 1.0 wt% antiwear additive AW3 on different base oils. Figure 6 shows the friction coefficient curves of lubricants containing 1.0 wt% AW3 under different load constant-speed and variable-speed tests. Figure 7 shows the typical morphology of steel-ball wear marks after constant- and variable-speed tests under different loads. According to Table 14, under constant- and variable-speed test conditions, the lubrication performance of different base oils is basically the same when the load is 198 N and 396 N. Based on the friction coefficient curve in Figure 6 and the analysis of the wear scar morphology of steel balls under different loads in Figure 7, it can be concluded that AW3 mainly plays a role as a friction modifier under light loads (198 N and 396 N). This reduces the actual contact area of the friction pair, resulting in a more similar morphology of the wear marks on different base oils. It is worth noting that in the constant- and variable-speed tests of 198 N, the friction coefficient of the mPAO4 base oil was significantly lower than that of other base oils. This is mainly due to the good lubrication performance of the mPAO4 base oil itself, combined with the surface physical adsorption of AW3, which enhances its film-forming ability. The exception is that the wear scar diameter of YU4 is significantly larger after the 396 N variable-speed test, which is mainly due to the poor shear resistance of the YU4 base oil itself.

Table 14. Sensitivity test results of different base oils containing antiwear additive AW3.

	1.0 wt% AW3				
	CTL4	YU4	GTL4	mPAO4	PAO4-M
$WSD_{196}^{1200} / \text{mm}$ (COF)	0.262 (0.077)	0.244 (0.070)	0.250 (0.065)	0.254 (0.062)	0.255 (0.083)
$WSD_{392}^{1200} / \text{mm}$ (COF)	0.364 (0.070)	0.368 (0.075)	0.361 (0.069)	0.363 (0.073)	0.360 (0.063)
$WSD_{795}^{1200} / \text{mm}$ (COF)	0.484 (0.076)	0.519 (0.081)	0.865 (Seizure)	>1.0 (Seizure)	0.526 (0.079)
$WSD_{196}^{0-2800} / \text{mm}$	0.268	0.264	0.257	0.259	0.268
$WSD_{392}^{0-2800} / \text{mm}$	0.391	0.526	0.398	0.360	0.383
$WSD_{795}^{0-2800} / \text{mm}$	0.697	0.684	0.681	0.683	0.705

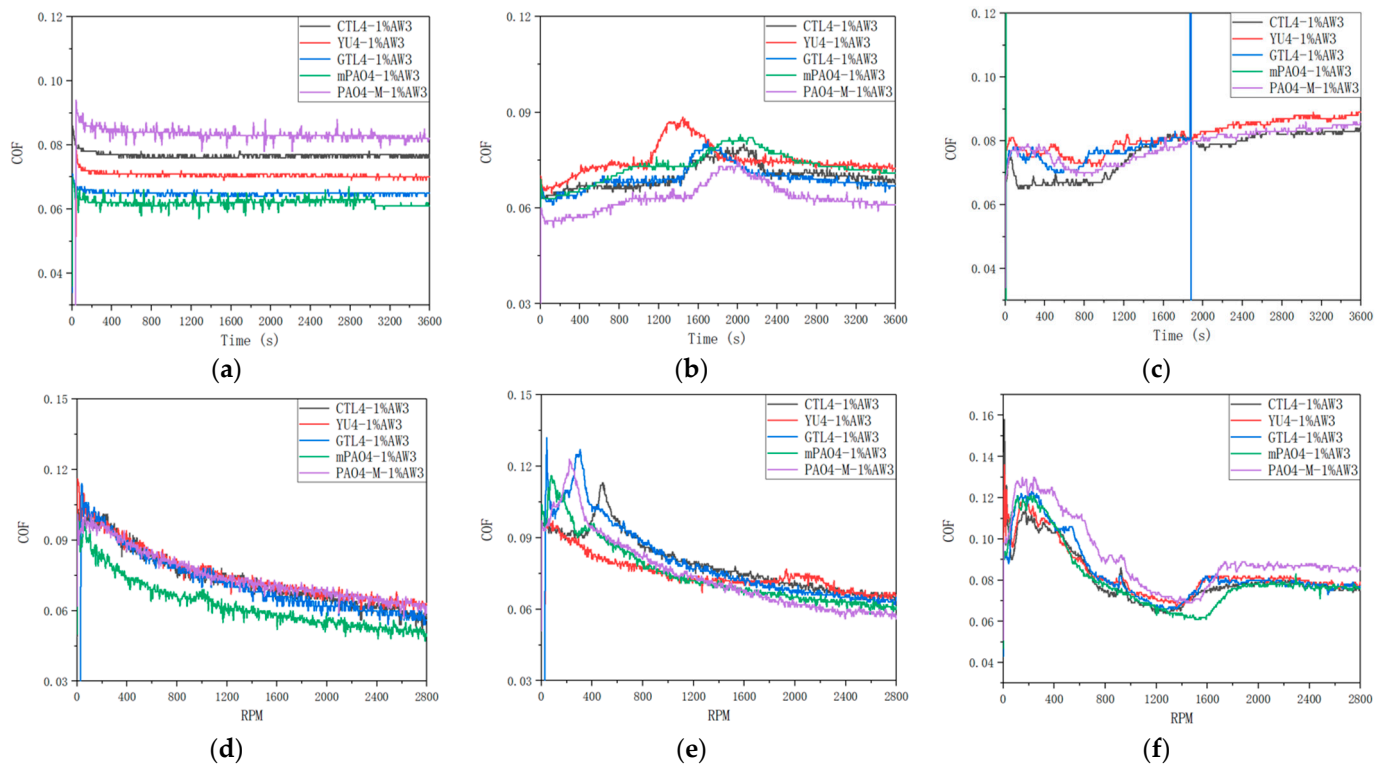


Figure 6. Friction coefficient curves of different base oils at different loads of 1.0 wt% AW3: (a) 198 N, 1200 rpm; (b) 396 N, 1200 rpm; (c) 792 N, 1200 rpm; (d) 198 N, 0–2800 rpm; (e) 396 N, 0–2800 rpm; (f) 792 N, 0–2800 rpm.

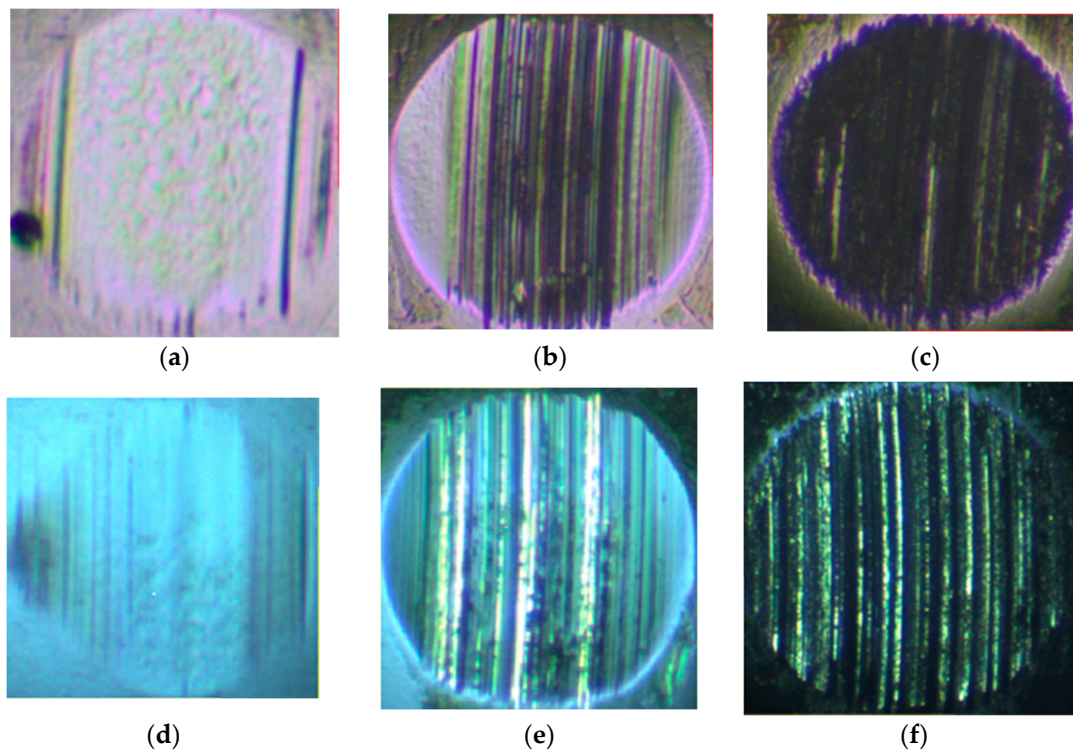


Figure 7. Typical morphology of steel-ball wear marks after constant- and variable-speed tests under different loads: (a) 198 N, 1200 rpm; (b) 396 N, 1200 rpm; (c) 792 N, 1200 rpm; (d) 198 N, 0–2800 rpm; (e) 396 N, 0–2800 rpm; (f) 792 N, 0–2800 rpm.

In the variable-speed test, the bearing capacity of the base oil is weaker when the speed is higher. There is a significant difference in the sensitivity of different base oils to 1.0 wt% AW3 under the constant-speed test conditions of a 792 N high load. After repeated experimental verification, the mPAO4 and GTL4 base oils show the seizure phenomenon (The green and blue curves in Figure 6c) during the start-up and midway stages of the test, indicating poor sensitivity to AW3, while the other base oils have similar sensitivity to the AW3 antiwear agents. In the 792 N high load variable-speed test, the friction coefficient of different base oils containing the 1.0 wt% AW3 antiwear agent experienced a trend of first decreasing, and then increasing, and then stabilizing with increasing speed. The decrease in the friction coefficient in the early stage is mainly caused by the increase in speed and the increase in the lubricating oil film thickness, which is related to the characteristics of the base oil itself. For example, if the film-forming ability of PAO4-M is poor, its friction coefficient is greater than other base oils during the speed increase process. As the rotational speed increases, the shear effect of the friction pair on the lubricant increases, and the oil film thickness decreases, increasing the friction coefficient. However, as the antiwear agent undergoes frictional chemical reactions with the metal surface, antiwear substances are generated on the surface of the friction pair, gradually stabilizing the friction coefficient. Among all the base oils containing the 1.0 wt% AW3 antiwear agent, the mPAO4 base oil reaches the highest speed of friction coefficient increase and has the lowest friction coefficient, which once again proves that mPAO4 has good oil film-forming ability and shear resistance.

4. Conclusions

In this study, the structure–property relationships of a variety of 4.0cSt base oils, including coal-to-hydroisomerization base oil (CTL4) and coal-to-poly-alpha-olefin base oil (mPAO4), and the sensitivity of typical antioxidants, extreme-pressure agents, and antiwear agents were studied. The main conclusions are listed as follows:

- (1) Compared to other hydroisomerization base oils, the composition distribution of CTL4 is more concentrated. Compared with GTL4, the overall branching degree of CTL4 is slightly lower, and the content of unbranched carbon in the molecule is higher. The CTL4 branched form is less and mainly methyl-branched. CTL4 has less branching at the end of the chain, and the branching concentration is slightly higher than that of GTL4;
- (2) Compared to commercially available PAO4-M base oil, mPAO4 base oil has less degree and type of isomerization, and there is no ethyl-branched chain isomerism in the isomeric form, resulting in a more regular molecular structure;
- (3) Compared to the GTL4 and YU4 base oils, the CTL4 base oil has better viscosity–temperature performance, low-temperature fluidity, fire safety, and evaporation loss. The lubricating properties of the three hydroisomerization base oils are similar. The physicochemical properties and lubricating properties of the mPAO4 base oil are better than those of commercial PAO4-M base oil;
- (4) There is no significant difference in the oxidation stability of different base oils. The sensitivity of different base oils to phenolic and amine antioxidants is better than that of sulfur antioxidants. The sensitivity of petroleum base oil and PAO base oil to typical antioxidants is better than that of coal- or natural gas-based hydroisomerization base oil;
- (5) The sensitivity of different base oils to typical extreme-pressure agents is slightly different, but the sensitivity to typical antiwear agents is different. The CTL4, GTL4, and mPAO4 base oils have better sensitivity to the AW1 antiwear agent. The sensitivity of CTL4 and mPAO4 to the AW2 antiwear additive was significantly better than PAO4-M. mPAO4 has a better sensitivity to reducing the friction coefficient of AW3;
- (6) The sensitivity of typical antioxidants and antiwear agents in the F-T synthetic base oil is generally lower than that of the mineral base oil and PAO base oil. It is necessary to develop new additives for F-T synthetic base oils.

Author Contributions: Conceptualization, J.L. (Junyi Liu) and Z.Z.; methodology, J.L. (Jiusheng Li) and R.P.; software, Z.Z.; validation, X.Z. and W.H.; formal analysis, X.Z.; investigation, J.L. (Jiusheng Li) and R.P.; resources, Z.Z.; data curation, X.Z.; writing—original draft preparation, Z.Z.; writing—review and editing, J.L. (Junyi Liu); visualization, J.L. (Junyi Liu); supervision, W.H.; project administration, X.Z. and R.P.; funding acquisition, J.L. (Jiusheng Li). All authors have read and agreed to the published version of the manuscript.

Funding: This research was funded by the 2021 Chinese Academy of Sciences Science and Technology Service Network Program (STS)-Dongguan Special Technology Innovation Project (20211600200042) and the Henan Province Science and Technology Research and Development Joint Fund (235101610007).

Data Availability Statement: The original contributions presented in the study are included in the article, further inquiries can be directed to the corresponding author.

Acknowledgments: Thank you to Shanxi Lu'an Taihang Lubrication Technology Co., Ltd. for providing base oils and some tests.

Conflicts of Interest: The authors declare no conflicts of interest.

References

1. Bart, J.C.J.; Gucciardi, E.; Cavallaro, S. 3—Lubricants: Properties and characteristics. In *Biolubricants*; Bart, J.C.J., Gucciardi, E., Cavallaro, S., Eds.; Woodhead Publishing: Cambridge, UK, 2013; pp. 24–73.
2. Sun, F. Technical progress of lubricant base oil production in China. *Energy Chem. Ind.* **2018**, *39*, 41–45.
3. Clark, R.H.; Wedlock, D.J.; Cherrillo, R.A. Future fuels and lubricant base oils from shell gas to liquids (GTL) technology. In *SAE Technical Paper 2005-01-2191*; SAE International: Warrendale PA, USA, 2005; pp. 1095–1110. [[CrossRef](#)]
4. Chen, C.; Tang, Q.; Xu, H.; Tang, M.; Li, X.; Liu, L.; Dong, J. Alkyl-tetralin base oils synthesized from coal-based chemicals and evaluation of their lubricating properties. *Chin. J. Chem. Eng.* **2023**, *58*, 20–28. [[CrossRef](#)]
5. Gatto, V.; Grina, M. Effects of base oil type, oxidation test conditions and phenolic antioxidant structure on the detection and magnitude of hindered phenol/diphenylamine synergism. *Tribol. Lubr. Technol.* **1999**, *55*, 11.
6. Giri, A.; Coutriade, M.; Racaud, A.; Stefanuto, P.H.; Okuda, K.; Dane, J.; Cody, R.B.; Focant, J.F. Compositional elucidation of heavy petroleum base oil by GC × GC-El/PI/CI/FI-TOFMS. *J. Mass Spectrom.* **2019**, *54*, 148–157. [[CrossRef](#)] [[PubMed](#)]
7. Kramer, D.C.; Ziemer, J.; Cheng, M.; Fry, C.E.; Reynolds, R.N.; Lok, B.K.; Sztenderowicz, M.L.; Krug, R.R. Influence of Group II & III base oil: Composition on VI and oxidation stability. *NLGI Spokesm.* **2000**, *63*, 20–39.
8. Korcek, S.; Jensen, R.K. Relation between Base Oil Composition and Oxidation Stability at Increased Temperatures. *ASLE Trans.* **1976**, *19*, 83–94. [[CrossRef](#)]
9. Yalin, Z.; Zhanquan, Z.; Yan, W.; Zhihua, Z. Comparative analysis of products from Fischer-Tropsch oil and petroleum based oil. *Chem. Ind. Eng. Prog.* **2018**, *37*, 3781–3787. [[CrossRef](#)]
10. Yinan, Y.; Liangcheng, A.; Xuemei, L.; Shudan, Z.; Yan, L.; Chun-hua, Z. Production Process of Coal-based Base Oil and Its Application in Lubricating Oil Products. *Contemp. Chem. Ind.* **2022**, *51*, 2989–2993. [[CrossRef](#)]
11. Hui, X.; Guoxu, C. Study on the oxidative stability of coal-to-liquid base oil using pressure differential scanning calorimetry method. *Lubr. Eng.* **2008**, *33*, 89–94. [[CrossRef](#)]
12. Liangcheng, A.; Xiaowen, Y.; Yan, L.; E, C.; Xuemei, L.; Chun-hua, Z.; Yi-nan, Y. Study on Sensitivity of GTL Base Oil and Antioxidant Additives. *Contemp. Chem. Ind.* **2023**, *52*, 579–583. [[CrossRef](#)]
13. Xuemei, L.; Yiwen, P.; Yinan, Y.; Chaolin, P.; Shudan, Z.; Yangyang, L.; Yan, L. Research on sensitivity of extreme-pressure and anti-wear additives in GTL base oil. *Lubr. Eng.* **2022**, *47*, 132–137. [[CrossRef](#)]
14. Huaqie, T.; Jianlin, S.; Zhao, H.; Daoxin, S.; Zhangliang, Z. Surface Lubrication and Adsorption Mechanism with Coal-to-Liquid as Aluminum Cold Rolling Base Oil. *Acta Pet. Sin. (Pet. Process. Sect.)* **2023**, *39*, 650. [[CrossRef](#)]
15. Yucheng, T.; Wei, H.; Zonggang, D.; Xian, F.; Lihua, Z. Driving Test of Coal-Based SN 5W-30 Gasoline Engine Oil. *Lubr. Eng.* **2023**, *48*, 207–212. [[CrossRef](#)]
16. Shoujing, G.; Tianzhong, B.; Xuemei, L.; Liangcheng, A.; Angui, Z. Research on blending of different base oils and application in diesel engine oil. *Pet. Refin. Eng.* **2021**, *51*, 53.
17. Zhang, C.; Wang, H.; Yu, X.; Peng, C.; Zhang, A.; Liang, X.; Yan, Y. Correlation between the Molecular Structure and Viscosity Index of CTL Base Oils Based on Ridge Regression. *ACS Omega* **2022**, *7*, 18887–18896. [[CrossRef](#)]
18. Yu, X.; Zhang, C.; Wang, H.; Wang, W.; Jiang, C.; Peng, C.; Yang, K. Oxidation degradation analysis of antioxidant added to CTL base oils: Experiments and simulations. *J. Therm. Anal. Calorim.* **2023**, *148*, 7033–7046. [[CrossRef](#)]
19. Xueqian, W.; Huixin, W. A Study into Using Olefin Made from Coal to Synthesize Low-Viscosity Poly-Alpha-Olefin Base Oil. *Sino-Glob. Energy* **2013**, *3*, 71–74. [[CrossRef](#)]
20. Huo, S.; Zhang, D.; Li, J.; Qian, J.; Yu, T. Study on the Technology of Preparing Polyalphaolefin Synthetic Oil from Coal-based Mixed Olefins. *J. Liaoning Univ. Pet. Chem. Technol.* **2022**, *42*, 24. [[CrossRef](#)]
21. Jian, X.; Jiusheng, L.; Junyi's, L. Synthesis Method of a Metallocene Catalyst. CN106543304A, 29 March 2017.

22. Ma, Y.; Xu, J.; Jiang, H.; Li, J. Low viscosity PAO preparation by oligomerization of alpha-olefin from coal with metallocene catalyst. *Pet. Process. Petrochem.* **2016**, *47*, 32–36. [[CrossRef](#)]
23. Ma, Y.; Xu, J.; Zeng, X.; Jiang, H.; Li, J. Preparation and performance evaluation of mPAO8 using olefin from coal as raw material. *Ind. Lubr. Tribol.* **2017**, *69*, 678–682. [[CrossRef](#)]
24. Sarpal, A.S.; Kapur, G.S.; Mukherjee, S.; Jain, S.K. Characterization by ¹³C nmr spectroscopy of base oils produced by different processes. *Fuel* **1997**, *76*, 931–937. [[CrossRef](#)]
25. Mäkelä, V.; Karhunen, P.; Siren, S.; Heikkinen, S.; Kilpeläinen, I. Automating the NMR analysis of base oils: Finding naphthene signals. *Fuel* **2013**, *111*, 543–554. [[CrossRef](#)]
26. *ASTM D445-24*; D02.07, Standard Test Method for Kinematic Viscosity of Transparent and Opaque Liquids (and Calculation of Dynamic Viscosity). ASTM International: West Conshohocken, PA, USA, 2024; p. 16.
27. *ASTM D2270-10R16*; D02.07, Standard Practice for Calculating Viscosity Index From Kinematic Viscosity at 40 °C and 100 °C. ASTM International: West Conshohocken, PA, USA, 2016; p. 5.
28. *ASTM D92-18*; D02.08, Standard Test Method for Flash and Fire Points by Cleveland Open Cup Tester. ASTM International: West Conshohocken, PA, USA, 2018; p. 11.
29. *ASTM D5950-02*; D02.07, Standard Test Method for Pour Point of Petroleum Products (Automatic Tilt Method). ASTM International: West Conshohocken, PA, USA, 2002; p. 5.
30. *ASTM D5293-20*; D02.07, Standard Test Method for Apparent Viscosity of Engine Oils and Base Stocks Between –10 °C and –35 °C Using Cold-Cranking Simulator. ASTM International: West Conshohocken, PA, USA, 2020; p. 12.
31. *ASTM D5800-21*; D02.06, Standard Test Method for Evaporation Loss of Lubricating Oils by the Noack Method. ASTM International: West Conshohocken, PA, USA, 2021; p. 25.
32. *ASTM D6186-19*; D02.09.0D, Standard Test Method for Oxidation Induction Time of Lubricating Oils by Pressure Differential Scanning Calorimetry (PDSC). ASTM International: West Conshohocken, PA, USA, 2019; p. 5.
33. *ASTM D2272-22*; D02.09.0C, Standard Test Method for Oxidation Stability of Steam Turbine Oils by Rotating Pressure Vessel. ASTM International: West Conshohocken, PA, USA, 2022; p. 22.
34. *GB/T 308.1-2013*; Rolling Bearing Balls Part 1: Steel Balls. General Administration of Quality Supervision, Inspection and Quarantine of the People’s Republic of China. China National Standardization Administration: Beijing, China, 2013; p. 20.
35. *GB/T 3142-2019*; Determination of Load-Bearing Capacity of Lubricants—Four Balls Method. State Administration for Market Regulation. China National Standardization Administration: Beijing, China, 2019; p. 20.
36. Lu, X.; Khonsari, M.; Gelinck, E. The Stribeck curve: Experimental results and theoretical prediction. *J. Tribol.* **2006**, *128*, 789–794. [[CrossRef](#)]
37. Höglund, E. The relationship between lubricant shear strength and chemical composition of the base oil. *Wear* **1989**, *130*, 213–224. [[CrossRef](#)]
38. Selby, T. The non-Newtonian characteristics of lubricating oils. *ASLE Trans.* **1958**, *1*, 68–81. [[CrossRef](#)]
39. Littlewood, A.B. *Gas Chromatography: Principles, Techniques, and Applications*; Elsevier: Amsterdam, The Netherlands, 2013.
40. Denis, J. The relationships between structure and rheological properties of hydrocarbons and oxygenated compounds used as base stocks. *J. Synth. Lubr.* **1984**, *1*, 201–238. [[CrossRef](#)]

Disclaimer/Publisher’s Note: The statements, opinions and data contained in all publications are solely those of the individual author(s) and contributor(s) and not of MDPI and/or the editor(s). MDPI and/or the editor(s) disclaim responsibility for any injury to people or property resulting from any ideas, methods, instructions or products referred to in the content.